Supporting Information

Characteristics of crystalline sputtered $LaFeO_3$ thin film for photoelectrochemical water splitting photocathode

Min-Kyu Son[1,4*], Hyunwoong Seo[2], Motonori Watanabe[1], Masaharu Shiratani[3,4], Tatsumi Ishihara[1]

[1]Molecular Photoconversion Devices Research Division, International Institute for Carbon-Neutral Energy Research (I^2CNER), Kyushu University, 744 Motooka, Nishi-ku, Fukuoka 819-0395, Japan
[2]Department of Energy Engineering, Inje University, 197 Inje-ro, Gimhae-si, Gyeongsangnam-do 50834, Republic of Korea
[3]Faculty of Information Science and Electrical Engineering, Kyushu University, 744 Motooka, Nishi-ku, Fukuoka 819-0395, Japan
[4]Center of Plasma Nano-interface Engineering, Kyushu University, 744 Motooka, Nishi-ku, Fukuoka 819-0395, Japan

*E-mail: minkyu.son@i2cner.kyushu-u.ac.jp

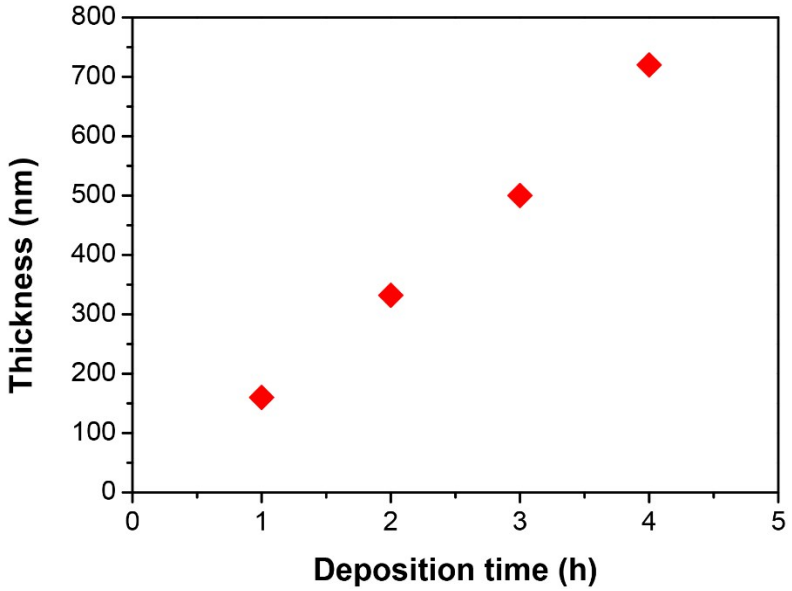

Figure S1. Thickness of sputtered $LaFeO_3$ film on Si wafer along with the deposition time.

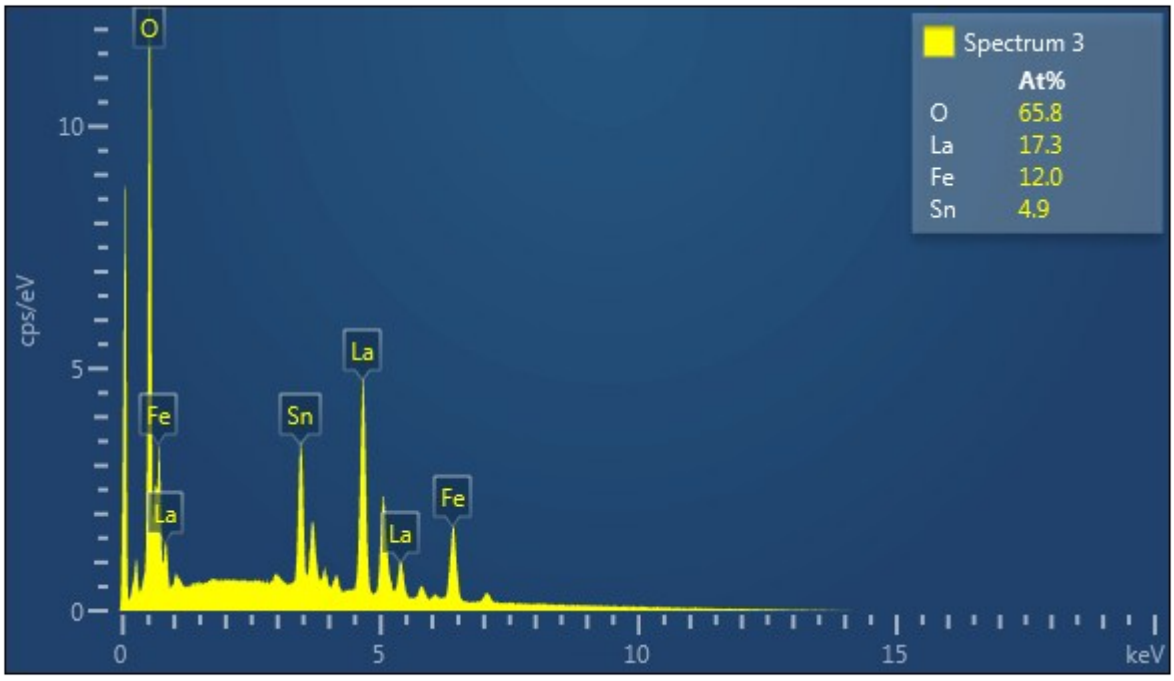

Figure S2. Compositional analysis of the crystalline sputtered $LaFeO_3$ film with post annealing process in air at 550 ℃ from EDX characterization.

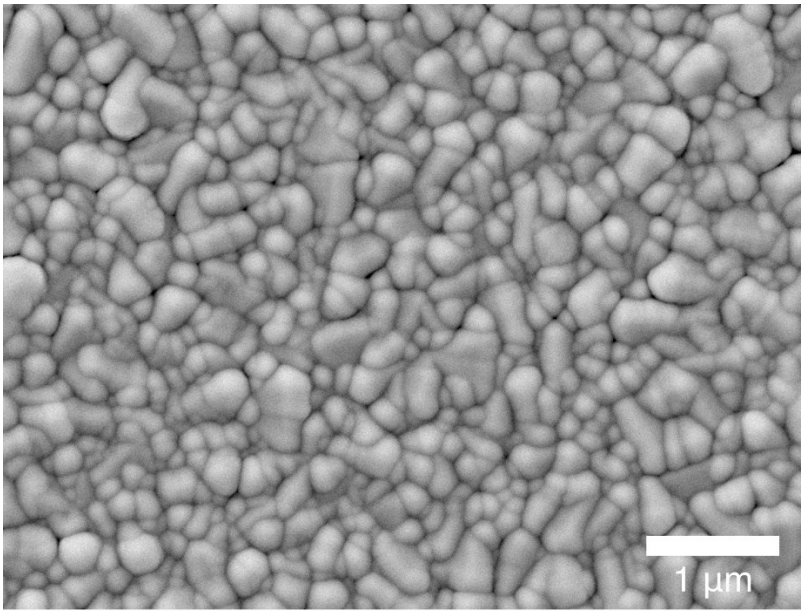

Figure S3. Top-view SEM image of the pristine sputtered $LaFeO_3$ film before post annealing process.

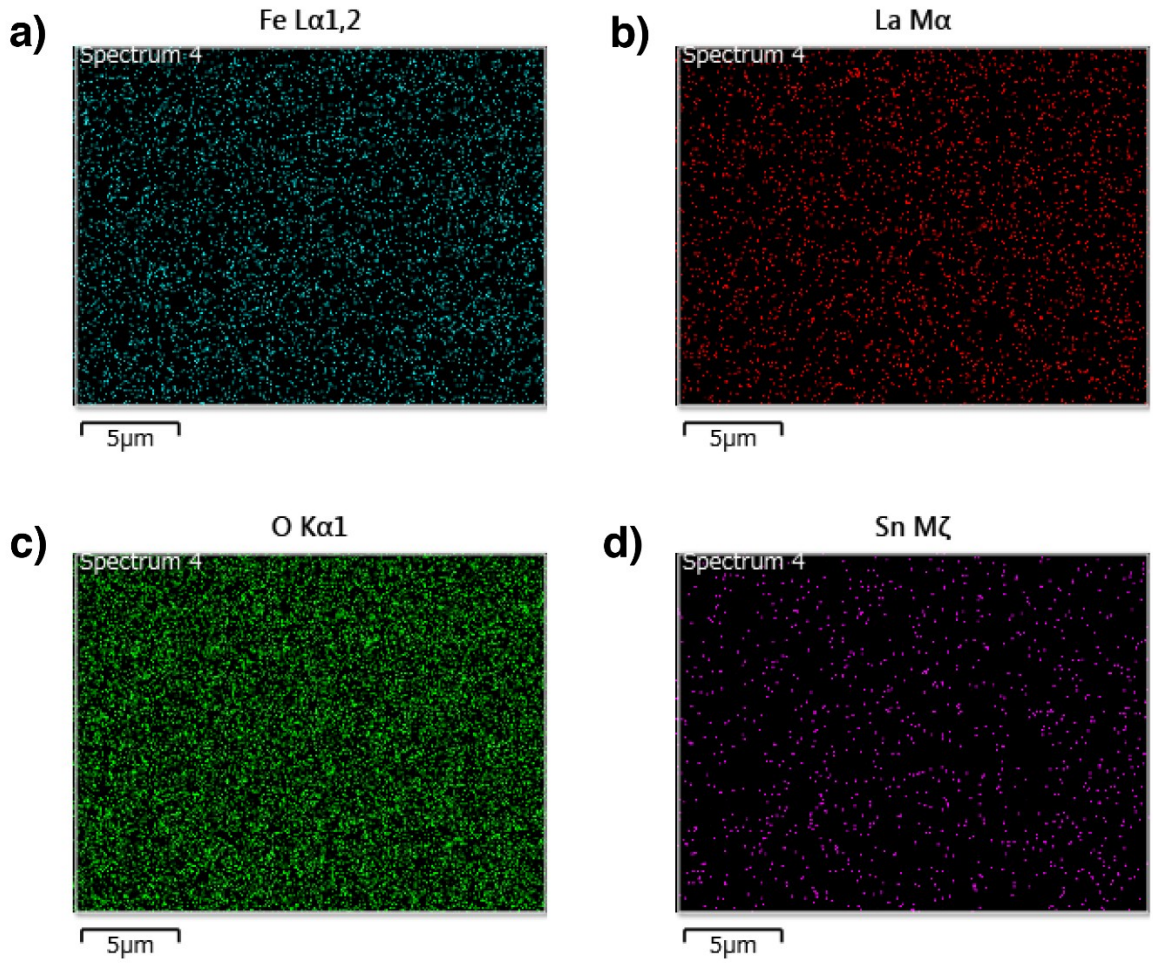

Figure S4. Element mapping of the crystalline sputtered $LaFeO_3$ film with post annealing process in air at 550 ℃ from EDX characterization: a) Fe, b) La, c) O and d) Sn, respectively.

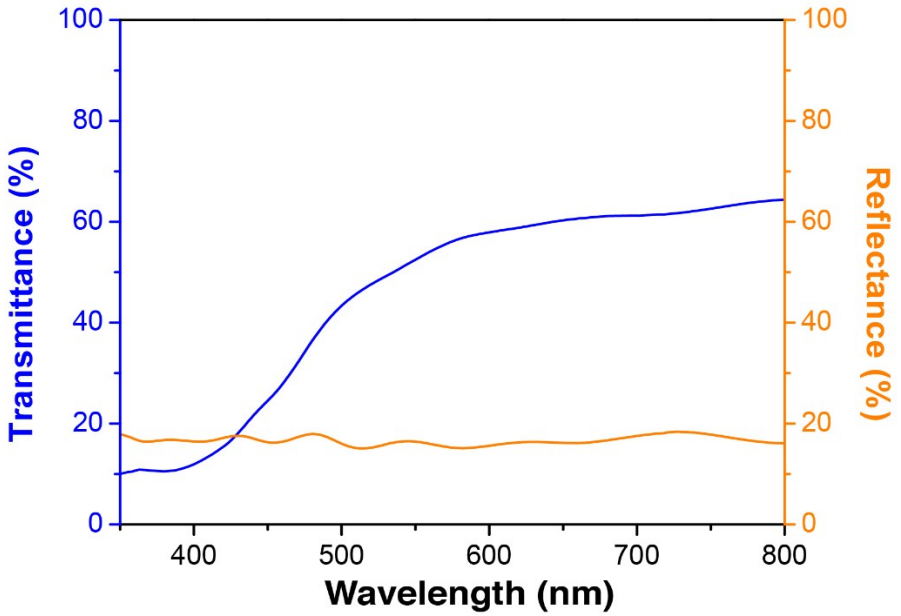

Figure S5. Transmittance and reflectance of the crystalline sputtered $LaFeO_3$ film on the FTO substrate.

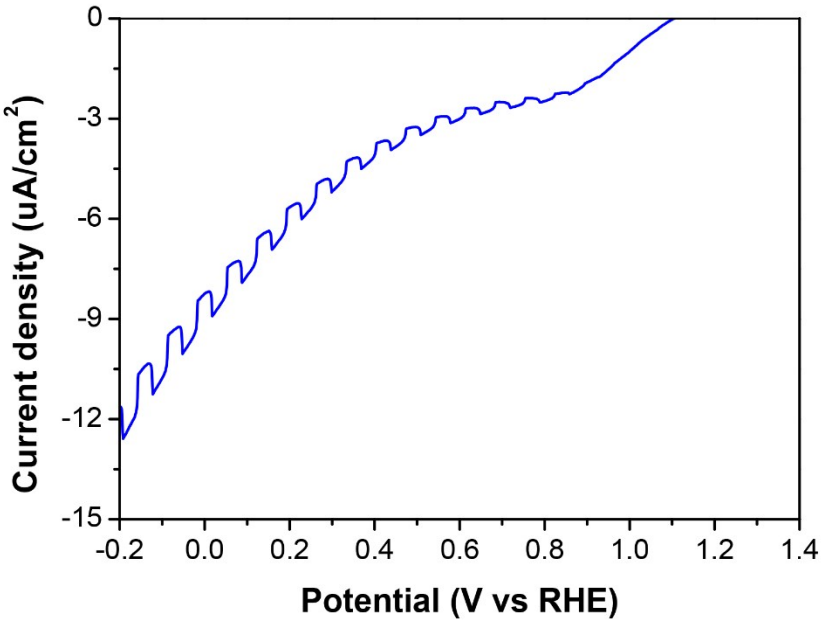

Figure S6. Current density-potential (J-E) characteristics of amorphous sputtered $LaFeO_3$ photocathode in strong alkaline solution (pH 13.6) under chopped one sun illumination.

Table S1. Photoelectrochemical performances of $LaFeO_3$ photocathode in other literatures and our work.

Fabrication method	Photocathode composition	Electrolyte	Current density ($\mu A\ cm^{-2}$)	Onset potential (V *vs* RHE)	Stability	*Ref.*
Electrodeposition	$LaFeO_3$	0.1 M NaOH saturated with O_2, pH 13 (0.1 M NaOH, pH 13)	-95 at 0.75 V *vs* RHE (-1.5 at 0.5 V *vs* RHE)	1.41 (1.27)	1 hr (1 hr)	23
Electrodeposition	K-doped $LaFeO_3$	0.1 M NaOH saturated with O_2, pH 13 (0.1 M NaOH, pH 13)	-268 at 0.6 V vs RHE (-11 at 0.6 V *vs* RHE)	1.2 (1.2)	15 hr (-)	24
Spray pyrolysis	$LaFeO_3$	0.1 M NaOH, pH 13	-160 at 0.26 V *vs* RHE	1.2	20 hr (20% decrease)	25
Spray pyrolysis	Ag incorporated $LaFeO_3$	0.1 M NaOH, pH 13	-74 at 0.6 V *vs* RHE	1.2	24 hr (5 % decrease)	26
Spray pyrolysis	Ni incorporated $LaFeO_3$	0.1 M NaOH, pH 13	-66 at 0.6 V *vs* RHE	1.2	20 hr	27
Sol-gel spin coating	$LaFeO_3$ with Au buffer layer	0.1 M Na_2SO_4, pH 7	-19 at 0.6 V *vs* RHE	1.0	50 min	28
Sol-gel spin coating	Ni-B catalysed $LaFeO_3$	0.1 M Na_2SO_4, pH 7	-23 at 0.6 V *vs* RHE	1.0	3.8 hr (82% decrease)	29
Spray pyrolysis	Dye-sensitized $LaFeO_3$ (NiP catalysed dye sensitized $LaFeO_3$)	1.0 M KOH saturated with O_2, pH 13.6 (0.5 M Na_2SO_4, pH 3)	-150 at 0.75 V *vs* RHE (-20 at 0.6 V *vs* RHE)	1.3 (1.1)	400 sec (400 sec, 20% decrease)	31
RF sputtering	$LaFeO_3$	0.1 M NaOH, pH 13.6	-25 at 0V *vs* RHE	1.3	30 min	Our work